DOI: 10.1002/ejic.200701135

The EDTA Complex of Oxidoiron(IV) as Realisation of an Optimal Ligand Environment for High Activity of FeO^{2+}

Leonardo Bernasconi*[a] and Evert Jan Baerends*[a]

Keywords: Alkane hydroxylation / High-valent oxidoiron systems / Fenton reaction / Density functional theory

A prerequisite for the high activity of the FeO^{2+} moiety as a hydroxylation agent is that its ligand environment stabilizes the $3\sigma^* \uparrow$ LUMO, which dominates the reactivity of this system. Features in the ligand environment that promote the reactivity of FeO^{2+} are: weak equatorial ligand field to obtain a quintet ground state that stabilizes the unoccupied $3\sigma^* \uparrow$; weak axial ligand field to stabilize the $3\sigma^* \uparrow$; a positive overall charge to lower the $3\sigma^* \uparrow$. Generalised gradient-corrected Density Functional Theory (DFT) calculations for the series of oxidoiron compounds of composition $[FeO{\cdot}EDTAH_n]^{(n-2)+}$, with $n = 0, 1, 2, 3, 4$, show that in particular the complex with $n = 4$ (charge +2) realises such an environment. Hypothetically, these species may appear as intermediates in the degradation of EDTA and related organics in aerated aqueous Fe^{II}/EDTA solutions. A strong dependence of the C–H activation properties in the hydroxylation of methane on the overall charge of yielding the lowest C–H dissociation barriers. In the $n = 4$ case, C–H dissociation occurs with an activation energy of ca. 7 kJ mol^{-1}, which is below the value computed for the corresponding reaction catalysed by $[FeO(H_2O)_5]^{2+}$ (23 kJ mol^{-1}). This enhanced catalytic activity is explained by $EDTAH_n^{(2-n)-}$ satisfying the listed requirements for an effective ligand, in particular by the very weak axial coordination by the EDTA nitrogen atoms due to large Fe–N distances.

Introduction

Oxidoiron(IV) (= ferryl) compounds have been the subject of a considerable amount of experimental and theoretical work, focussing on their role as key intermediates in biological and biomimetic oxidations,[1–15] in which they act as catalysts for the hydroxylation of saturated hydrocarbons. A number of artificial non heme ferryl complexes of composition $[FeO{\cdot}L_5]^z$ (with z being the ionic charge) have been synthesised and chemically characterised since 2000 (see, for instance, ref.[16–22]). The intriguing electronic and spectroscopic properties of some of these compounds have also been addressed in several theoretical studies[23–29] which have highlighted an important link between spin state and reactivity in hydroxylation catalysis.[30–32] In particular, it is now well established that for reactions carried out in vitro, as a rule, quintet ("high-spin") *non-heme* oxido-Fe^{IV} compounds are substantially more active in hydroxylations than triplet ("intermediate-spin") ones.

Rather surprisingly from this perspective, the vast majority of the artificial non-heme systems synthesised to date are triplet compounds, in which a $[FeO]^{2+}$ group is stabilised by one or more (nitrogen-based) ligands. As recently pointed out,[33] the reactivity of some of these complexes (see, for instance, Scheme 1c in ref.[33]) is not necessarily dominated by the triplet state alone. A crossing to the quintet state, possibly occurring en route as the hydroxylation proceeds, may have important implications on the catalytic activity of these species, as well as on the reaction mechanism (concerted vs. stepwise), stereoselectivity, and on the reaction dependence on solvent effects. The complex patterns exhibited by hydroxylation reactions involving "triplet" oxidoiron compounds thus reflects the underlying two-state reactivity, and the different modalities by which this may be brought about.

Much less is known regarding the reactivity of synthetic quintet oxidoiron compounds, and at present pentaaqua oxidoiron $[FeO(H_2O)_5]^{2+}$, which was obtained by reaction of O_3 and aqueous Fe^{II},[34–36] is the only compound from this category which has been fully characterised chemically and spectroscopically. This species was found to be stable over a period of about 10 seconds, and to behave as a strong oxidant acting in both one-electron hydrogen abstractions and two-electron oxidations of alcohols to ketones.[35] $[FeO(H_2O)_5]^{2+}$ has also been proposed as a possible active species in organic reactions catalysed by the Fenton reagent, aqueous H_2O_2/Fe^{II}.[8,25,37–41] We have recently presented a study of the relation between reactivity, spin state and electronic structure of oxido-Fe^{IV} complexes derived from $[FeO(H_2O)_5]^{2+}$ by progressive substitution of the

[a] Theoretische Chemie, Vrije Universiteit Amsterdam
De Boelelaan 1083, 1081 HV Amsterdam, The Netherlands
Fax: +31-20-598-7629
E-mail: L.Bernasconi@few.vu.nl
EJ.Baerends@few.vu.nl

Supporting information for this article is available on the WWW under http://www.eurjic.org or from the author.

water ligands.[42] Our work was based on DFT calculations performed on small gas-phase clusters, and was aimed at extending earlier findings about the importance of a low lying $3\sigma^* \uparrow$ orbital in influencing the reactivity of $[FeO(H_2O)_5]^{2+}$ in alkane hydroxylations.[25,41,43,44] Our main conclusions can be summarised as follows.

In simple complexes of composition $[FeO(H_2O)_n(L)_{5-n}]^{2+}$ with L = NH_3, CH_3CN, H_2S, BF_3 and n = 4, 1, 0, the ground state is either a quintet (S = 2) or a triplet (S = 1). These two spin states are very close in energy, and the quintet state is always more reactive than the triplet. The preference for the quintet ground state over the triplet is determined by the strength of the *equatorial ligand field* (i.e. by the electron-donor properties of ligands roughly located in a plane perpendicular to the Fe–O bond): stronger donors, e.g. N-based ligands, tend to favour the triplet state. A quintet ground state is observed in the presence of O-based ligands, as in $[FeO(H_2O)_5]^{2+}$. The axial ligand has a comparatively modest, but not negligible, influence on the reactivity of a complex in the quintet state. Electron donors stronger than H_2O yield systems with reduced catalytic activity compared to $[FeO(H_2O)_5]^{2+}$.

These findings can be rationalised based on the observation that the ability of a ferryl system to promote saturated C–H bond breaking, which is the first step of the rebound mechanism[8,45,46] for organic hydroxylations, is strongly dependent on the electrophilic character of the ferryl-O group. In the quintet state this is much enhanced by the presence of an empty $3\sigma^* \uparrow$ orbital at very low energy (see discussion in ref.[43]), acting as a one-electron acceptor during the transfer of an H atom from the substrate to the catalyst. In the triplet state, this orbital is destabilised by reduced exchange interaction, and electron donation from the substrate occurs through alternative, and less efficient, paths. The latter situation is common in heme and heme-like ferryl complexes. The residual influence on the reactivity from the axial ligand is explained by the same principle: strong donors destabilise the $3\sigma^* \uparrow$ orbital and therefore reduce the electron-acceptor ability of the ferryl moiety. For a hypothetical quintet ferryl complex with a vacant axial coordination site we computed a virtually vanishing energy for H-abstraction from methane, to be compared to a barrier of 23 kJ mol^{-1} in the corresponding reaction catalysed by $[FeO(H_2O)_5]^{2+}$. Whereas the methane hydroxylation by way of the rebound mechanism is widely accepted for the ferryl group in P450 and similar fully coordinated (biomimetic) species, the possibility of a nonradical mechanism for the bare FeO^+ species has also received much attention.[47]

The involvement of a high valent ferryl (Fe^{IV}) or perferryl (Fe^{V}) species has been invoked in recent studies on the autoxidation reaction of Fe^{II} in the presence of ethylenediaminetetraacetate (EDTA) and other chelating ligands.[48–50] Experimental evidence has been put forward for the generation of a strong oxidant, responsible for the degradation of the ligand and the associated organics, whose reactivity differs from the one of a hydroxyl radical. It has been proposed that $[FeO(H_2O)_5]^{2+}$ may be generated in experimental conditions as a by-product of the Fe^{II}-to-Fe^{III} oxidation. According to the autoxidation mechanism proposed by van Eldik and coworkers,[51,52] H_2O_2 is produced by the donation of two electrons from two chelated Fe^{II} ions to a dioxygen molecule, followed by diprotonation. Englehardt et al. advanced the hypothesis that the H_2O_2 thus generated may initiate a chain of reactions whose ultimate product is (solvated) $[FeO(H_2O)_5]^{2+}$; see Equations (1), (2), (3).

$$H_2O_2 + [Fe^{II}\cdot(H_2O)_6]^{2+} \rightarrow [Fe^{II}\cdot(H_2O)_5(H_2O_2)]^{2+} + H_2O \quad (1)$$

$$[Fe^{II}\cdot(H_2O)_5(H_2O_2)]^{2+} \rightarrow [Fe^{IV}\cdot(H_2O)_4(OH)_2]^{2+} + H_2O \quad (2)$$

$$[Fe^{IV}\cdot(H_2O)_4(OH)_2]^{2+} + H_2O \rightarrow [Fe^{IV}O(H_2O)_5]^{2+} + H_2O \quad (3)$$

The plausibility of the process described by these reactions had been put forward in computational studies based on DFT and ab initio molecular dynamics simulations.[25,41,53]

As an alternative route to ferryl species in EDTA chelated Fe^{II} solutions, which is also fully consistent with the van Eldik autoxidation mechanism, we have explored theoretically the formation of *chelated* $[Fe^{IV}O]^{2+}$ from direct homolytic cleavage of a dioxygen molecule coordinated to two (monoprotonated) $[Fe\cdot EDTAH]^-$ units[54]; see Equation (4), note that O_2 is formally a *peroxo* bridge.

$$[(EDTAH)Fe^{III}(O_2)Fe^{III}(EDTAH)]^{2-} \rightarrow 2\,[Fe^{IV}O\cdot(EDTAH)]^- \quad (4)$$

Reductive O–O cleavage is known to occur in enzymes containing dinuclear non-heme iron sites responsible for O_2 activation.[55–57] Besides, theoretical studies suggest that high valent iron compounds may be generated through homolytic O–O breaking, as in e.g. methane monooxygenase, ribonucleotide reductase[58–60] and tyrosinase,[61] with overall dissociation barriers similar to the cleavage of the dinuclear complex appearing in the last reaction above (ca. 70 kJ mol^{-1}; see ref.[54] for further details).

What makes the latter reaction pathway so appealing, according to the analysis of ref.[42], is that the metal ion coordination in the resulting FeO/EDTA complexes possesses two crucial features promoting the activity of the ferryl group as a hydroxylation catalyst, namely *(a)* a weak (oxygen-rich) equatorial ligand environment (see Figures 1 and 2), which stabilises the quintet ground state over the triplet and *(b)* the absence of a proper axial donor ligand *trans* to the oxo group, which is replaced by the two nitrogen atoms of the EDTA framework. As will be shown below the latter are typically located at considerably larger distances than, e.g., the axial water molecule in $[FeO(H_2O)_5]^{2+}$. Therefore the axial region of the ferryl group is relatively unhindered, free from strong electron-donor ligands, and protected from attack of solvent molecules by the presence of the ligand cage. The central issue that we address in this work is whether these features may be sufficient to yield a (gas phase) compound with C–H activation properties *superior* to those of $[FeO(H_2O)_5]^{2+}$. We pay particular attention to the dependence of the catalytic activity on the overall charge of the FeO/EDTA catalyst, which is in turn the result of the protonation state of the EDTA ligand. Accord-

ing to the results described here, good catalytic efficiency is only achievable for a fully protonated complex, which, as will be shown, follows as a direct consequence of some of the arguments regarding the orbital structure of ferryl complexes of ref.[42,43]

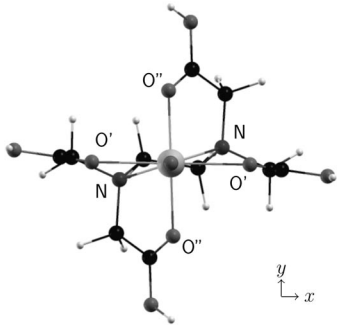

Figure 1. Structure of the fully protonated complex of EDTA with FeO^{2+}, $[FeO{\cdot}EDTAH_4]^{2+}$, seen along the FeO axis (conventionally indicated as the z axis). The Fe^{IV} ion is at the plot centre. O′ and O′′ indicate coordinating oxygens wich are roughly in plane with the N atoms and roughly perpendicular to the N–N direction respectively. The x and y axes are oriented approximately along the O′–O′ and O′′–O′′ directions, respectively.

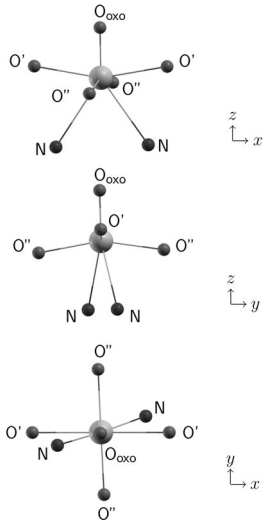

Figure 2. Schematic representations of the FeIV coordination geometry in $[FeO{\cdot}EDTAH_4]^{2+}$, with the axis labelling used in this work. The orientation of the third panel is the same as in Figure 1, i.e. the two N atoms are behind the Fe atom and the O atom and the oxo group is in front of the Fe atom.

Computational Details

DFT calculations were performed using ADF[62–64] with a basis set of Slater type orbitals of TZ2P quality for all atomic species. Relativistic effects were included using the Zero-Order Regular Approximation (ZORA).[65] Calculations were carried out at the BLYP[66,67] and OPBE[68,69] levels of theory. The latter exchange-correlation functional has been shown to yield relative stabilities of different spin states of various inorganic and organometallic iron complexes of accuracy comparable to hybrid and some *meta*-GGA functionals.[70–73] The recent results of Hirao et al.[33] also points to a general agreement between OPBE and B3LYP in predicting the most stable spin state of various FeO complexes, although the triplet-quintet splitting appears to be somewhat underestimated by OPBE. BLYP results have been included here for consistency with previous work. We observe that, in all cases examined here, OPBE and BLYP yield the same spin multiplicity for the ground state of a given complex. Convergence criteria for geometry optimisations were 5×10^{-4} hartree in the total energy, 5×10–3 hartree/Å in the gradients, 5×10^{-3} Å in bond lengths and 0.25 degrees in bond and dihedral angles.

Results and Discussion

Equilibrium Geometries and Electronic Structures

The protonation of one or more carboxylic arms of $[FeO{\cdot}EDTA]^{2-}$ gives rise to a series of charged or neutral complexes of composition $[FeO{\cdot}EDTAH_n]^{(n-2)+}$, with n = 0, 1, 2, 3, 4 the protonation number of the complex. The added proton was always found to bind preferentially to the non coordinating oxygen atom of a given carboxylic group which is at larger distance from the metal centre. Different choices of protonation states are compatible with the cases n = 1, 2 and 3. It is convenient to indicate as O' and O'' those pairs of coordinating oxygens of carboxylic arms lying roughly along the x axis in plane with the two nitrogen atoms, and along the y axis perpendicular to the NNO′O′′ plane, respectively (see Figure 1 for $[FeO{\cdot}EDTAH_4]^{2+}$). A simplified representation of the FeO coordination geometry in $[FeO{\cdot}EDTAH_4]^{2+}$ and our convention for the Cartesian axes are shown in Figure 2. Notice that in the present work we label z axis the direction of the $Fe–O_{oxido}$ bond. Assuming that carboxylic arms belonging to the same pair (i.e. *trans* to each other with respect to the metal ion) constitute equivalent protonation sites, two alternative protonation patterns are possible for n = 1, 2, 3, namely O' or O'' for n = 1, $2O'$ or $2O''$ for n = 2 (we do not consider here simultaneous protonation of sites which are *cis* to each other), and $2O',O''$ or $2O'',O'$ for n = 3. We optimised the structure of each of the resulting 8 complexes (including the fully protonated and fully unprotonated ones) in the high (quintet) and intermediate (triplet) spin states at the BLYP and OPBE levels of theory. In all cases we found the quintet state to be lowest in energy by 49–86 $kJ\,mol^{-1}$ (Table 1). A much lower difference in energy between the two spin states (ca. 1 $kJ\,mol^{-1}$) was only observed in the case of $[FeO{\cdot}EDTAH]^-$ (OPBE). Both functionals were found to favour O', $2O'$ and $2O'',O'$ protonation for n = 1, 2 and 3 respectively.

The total energy of a complex depends non-monotonically on the protonation number (Figure 3), with low protonation numbers n = 1–3 favourite compared to both the unprotonated and the fully protonated cases. This trend is understandable considering the effect of protonating one or more carboxylic arms on the geometry of the complex

Table 1. Energy difference (in kJ mol^{-1}) between optimised triplet and quintet state structures. For n = 1, 2 and 3 only the most stable protonation patterns are listed.

	BLYP	OPBE
$[FeO{\cdot}EDTA]^{2-}$	74	64
$[FeO{\cdot}EDTAH]^{-}$	60	1
$[FeO{\cdot}EDTAH_2]$	77	49
$[FeO{\cdot}EDTAH_3]^{+}$	62	61
$[FeO{\cdot}EDTAH_4]^{2+}$	10	85

(Table 2). As we observed elsewhere[54] for the case of Fe^{2+}/EDTA complexes, protonation reduces the affinity of a carboxylic arm for the metal ion. This originates from the reduction of structural strain in the ligated EDTA caused by the protonated arm moving away from the metal centre to an arrangement which is more similar to the one of the free ligand; see, for instance, the increase in the Fe–O′ distance from 2.0–2.2 Å to ca. 4.1 Å upon protonation, and of the Fe–O′′ to ca. 2.5 Å (BLYP) and ca. 2.8 Å (OPBE). To counterbalance the change in the electrostatic field of the coordinating environment, the metal ion moves off the ligand cage centre closer to the remaining unprotonated arms. The distance between the Fe^{IV} ion and the negative carboxylate groups is for instance reduced from ca. 2.1 to 2.0 Å in the case of single protonation, which lowers the overall symmetry of the complex. A further reduction to ca. 1.9 Å between Fe^{IV} and the unprotonated *O′′* carboxylates is observed in $[FeO{\cdot}EDTAH_2]$. Rather unexpectedly, protonated carboxylic arms in the optimised n = 3 and 4 complexes do not show a tendency to move away from the metal ion. This might be a consequence of the fact that, at higher protonation, the gain in energy from structural relaxation is insufficient to compensate the reduced bonding between carboxylic groups and the metal ion. At n = 4 the electrostatic stabilisation of FeO^{2+} interacting with negatively charged carboxylate groups is virtually lost, but a complete relaxation to the free-ligand structure is prevented by orbital interactions of carboxylic oxygens and Fe^{IV}. Overall the relative stability of a give complex is therefore the resultant of at least three factors: (1) metal ion/ligand electrostatic attraction, dominant at low n; (2) ligand strain relaxation, more favourable at intermediate n; (3) orbital interaction, virtually contributing for all values of n, but

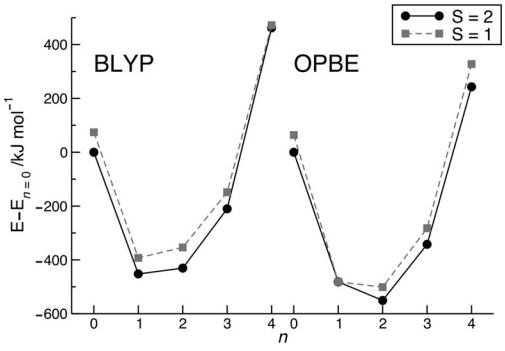

Figure 3. Total energy of optimised $[FeO{\cdot}EDTAH_n]^{(n-2)+}$ in the high (S = 2) and intermediate (S = 1) spin states, as a function of the protonation number n, obtained at the BLYP and OPBE levels of theory. Values reported here are relative to the energy of the high spin *unprotonated* complex. For n = 1, 2 and 3 only the energy of the most stable protonation patters, O′,2O′ and 2O′′,O′, respectively, is shown.

Table 2. Selected parameters from BLYP- and OPBE-optimised geometries of high-spin $[FeO{\cdot}EDTAH_n]^{(n-2)+}$. For n = 1–3, the protonation patterns alternative to the most stable one are shown in the bottom columns. The latter are 161, 69 and 12 (BLYP) and 108, 84 and 12 kJ mol^{-1} (OPBE) higher in energy than the corresponding alternative protonation patterns for n = 1, 2 and 3, respectively. Distances are given in Å, angles in degrees.

	$[FeO{\cdot}EDTA]^{2-}$		$[FeO{\cdot}EDTAH]^{-}$ *O′*		$[FeO{\cdot}EDTAH_2]$ *2O′*		$[FeO{\cdot}EDTAH_3]^{+}$ *2O′,O′′*		$[FeO{\cdot}EDTAH_4]^{2+}$	
	BLYP	OPBE	BLYP	OPBE	BLYP	OPBE	BLYP	OPBE	BLYP	OPBE
FeO(oxido)	1.650	1.632	1.648	1.625	1.653	1.618	1.651	1.615	1.633	1.633
FeO′	2.087, 2.091	2.124, 2.119	4.154, 2.049	4.136, 2.049	3.068, 3.068	3.008, 3.004	4.034, 2.254	3.859, 2.286	2.271, 2.204	2.234, 2.235
FeO′′	2.083, 2.080	2.100, 2.107	1.997, 2.002	2.007, 2.004	1.915, 1.915	1.899, 1.889	2.168, 1.896	2.144, 1.865	2.053, 2.046	2.049, 2.049
FeN	2.888, 2.901	2.858, 2.848	2.200, 2.589	2.207, 2.597	2.370, 2.370	2.413, 2.413	2.386, 2.238	2.251, 2.429	2.616, 2.716	2.671, 2.672
O′FeO′	168.99	168.49	155.31	157.06	157.16	160.41	147.19	147.58	160.49	160.81
O′′FeO′′	141.91	144.28	153.28	153.36	164.66	163.57	165.31	165.77	160.78	161.26
NFeN	61.83	62.46	78.50	77.55	80.12	76.98	81.93	79.67	68.18	68.11
	$[FeO{\cdot}EDTAH]^{-}$ *O′*		$[FeO{\cdot}EDTAH_2]$ *2O′′*		$[FeO{\cdot}EDTAH_3]^{+}$ *2O′′,O′*					
	BLYP	OPBE	BLYP	OPBE	BLYP	OPBE				
FeO(oxido)	1.667	1.629	1.655	1.619	1.655	1.617				
FeO′	2.002, 1.988	1.970, 1.954	1.940, 1.948	1.919, 1.920	4.112, 1.898	4.112, 1.881				
FeO′′	2.485, 2.009	2.854, 1.992	2.284, 2.328	2.340, 2.366	2.270, 2.260	2.230, 2.921				
FeN	3.166, 2.988	3.308, 3.018	3.081, 3.030	3.136, 3.109	2.280, 2.220	2.350, 2.220				
O′FeO′	170.52	163.71	170.09	176.37	145.92	149.19				
O′′FeO′′	132.92	131.30	135.82	136.14	159.31	159.60				
NFeN	57.87	56.14	58.57	57.07	83.45	81.07				

likely to be strongly influenced by changes in the local coordination geometry of the metal ion brought about by the ligand distortion. For a detailed analysis of the orbital interaction in related Fe^{II}/EDTA complexes, see ref.[54].

The electronic structure of all complexes examined here retains various distinctive features of most quintet FeO systems studied to date. As an example, the one particle energy spectrum of $[FeO{\cdot}EDTAH_4]^{2+}$ is shown in Figure 4, and a selected number of Kohn–Sham eigenvalues for each complex are collected in Table 3. Apart from possible charge-dependent energy shifts, the ordering and spatial distribution of ferryl states is analogous to other quintet ferryl systems in the gas phase[25,29,42,43,74] and in solution.[25,41,43] Note the double occupancy of the Fe–O bonding 2σ, $1\pi_x$ and $1\pi_y$ and the four singly occupied $2\pi_x\uparrow$, $2\pi_y\uparrow$, $1\delta_{xy}\uparrow$ and $1\delta_{x^2-y^2}\uparrow$, which creates a strongly stabilizing exchange potential pulling the up spin $3\sigma^*\uparrow$ very much down compared to the down spin $3\sigma^*\downarrow$. States (of either spin) in the low energy region of the virtual spectrum dominate the reactivity of Fe^{IV} compounds in organic hydroxylations, in which they act as acceptors of one electron from a substrate. $1\delta_{xy}\downarrow$ and $1\delta_{x^2-y^2}\downarrow$ do not contribute to the interaction with the substrate, as they extend in the *xy* plane, i.e. perpendicular to the direction of attack to the ferryl ion, which is at the oxo group. In quintet ferryl compounds, $3\sigma^*\uparrow$, $2\pi_x\downarrow$ and $2\pi_y\downarrow$ (Figure 5) can all play a role in the electron transfer. Depending on the relative energy of the $3\sigma^*\uparrow$ and the $2\pi_{x,y}\downarrow$ pair *relative to the donor orbital of the substrate*, the substrate/catalyst interaction may be a pure donor→$3\sigma^*\uparrow$, donor→$2\pi_{x,y}\downarrow$, or a combination of the two. It appears that for energy differences of the order of 1 eV or more between $3\sigma^*\uparrow$ and $2\pi_{x,y}\downarrow$, the interaction involves only the lower energy orbital(s).[43] In all cases examined here, the $3\sigma^*\uparrow$ orbital is 0.6–1.1 eV lower than the $2\pi_{x,y}\downarrow$ (see last column of Table 3), and, as will be shown below, the donor orbital is always at least ca. 1.6 eV more stable than the $3\sigma^*\uparrow$, once the reactants are at interaction distance. Therefore, the reactivity of all the systems studied here may be considered to originate exclusively from the $3\sigma^*\uparrow$ channel, as it is likely to be the case in e.g. gas-phase or solvated-phase reaction catalysed by $[FeO(H_2O)_5]^{2+}$.

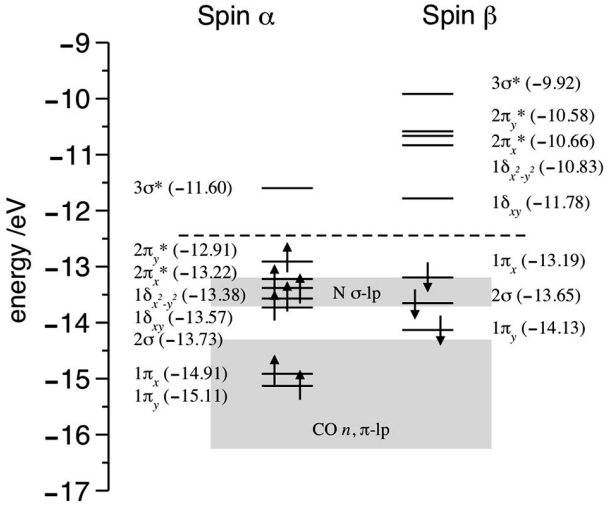

Figure 4. Selected OPBE Kohn–Sham levels of the ferryl ion in $[FeO{\cdot}EDTAH_4]^{2+}$. One particle energies are indicated in parenthesis. Shaded areas represent energy ranges spanned by the N σ lonepairs, and by the carbonyl *n* and π lonepairs. The dashed line separates virtual from occupied states.

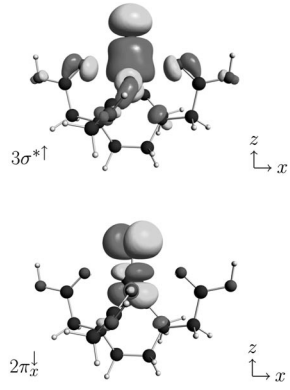

Figure 5. Virtual low energy Kohn–Sham orbitals of $[FeO{\cdot}EDTAH_4]^{2+}$, which can act as electron acceptors in hydroxylations. Projections are shown in (approximately) the *xz* plane, with the *z* axis along the vertical. The $2\pi_y^*\downarrow$ orbital has analogous shape and symmetry to the $2\pi_x^*\downarrow$ and it is oriented perpendicular to it.

Catalytic Properties

Within the rebound mechanism scenario,[8,45,46] the abstraction of a hydrogen atom from a substrate RCH to yield a carbon radical [R–C↑] and a cation $[FeO\text{-}H\uparrow]^{2+}$ has been identified as the first step of the conversion of a hydrocarbon to the corresponding alcohol. The reaction, both in

Table 3. OPBE Kohn–Sham orbital energies (in eV) for optimised $[FeO{\cdot}EDTAH_n]^{(n-2)+}$ complexes. For systems with alternative protonation patterns, only the most stable species is considered (see also Table 2); note the large positive energy caused by a negative charge on the complex. The difference in energy between the $2\pi_x^*\downarrow$ and the $3\sigma^*\uparrow$ orbitals is shown in the rightmost column; see text for the significance of these values.

	$1\delta_{x^2-y^2}\uparrow$	$2\pi_x^*\uparrow$	$2\pi_y^*\uparrow$	$3\sigma^*\uparrow$	$1\delta_{xy}\downarrow$	$1\delta_{x^2-y^2}\downarrow$	$2\pi_x^*\downarrow$	$2\pi_y^*\downarrow$	$\Delta(2\pi_x^*\downarrow, 3\sigma^*\uparrow)$
$[FeO{\cdot}EDTA]^{2-}$	1.046	1.144	1.227	2.301	2.522	3.283	3.442	3.573	1.141
$[FeO{\cdot}EDTAH]^{-}$	–2.317	–2.168	–1.846	–0.414	–0.484	0.023	0.283	0.552	0.697
$[FeO{\cdot}EDTAH_2]$	–6.021	–5.569	–5.486	–3.895	–4.351	–3.953	–3.140	–3.059	0.755
$[FeO{\cdot}EDTAH_3]^{+}$	–9.451	–9.296	–9.084	–7.513	–7.848	–7.166	–6.874	–6.598	0.639
$[FeO{\cdot}EDTAH_4]^{2+}$	–13.378	–13.219	–12.909	–11.598	–11.782	–10.833	–10.665	–10.584	0.933

solution and (hypothetically) in the gas phase, is initiated by the formation of a weakly bound encounter complex, $[FeO]^{2+}$–[HCR] in which a dative bond of type $\sigma(CH)\rightarrow 3\sigma^*\uparrow$ exists between the substrate and the ferryl catalyst.[43] The strength of the interaction is proportional to the amount of mixing between the donor orbital of the substrate and the acceptor orbital of the oxidoiron catalyst, which is typically very small in the encounter complex and increases as the reaction proceeds on to the breaking of the C–H bond. This pathway was observed in the reaction of aqueous $[FeO(H_2O)_5]^{2+}$ with methane and methanol,[41,75] and in the reaction of gas-phase $[FeO(H_2O)_n(L)_{5-n}]^{2+}$ with (L = NH_3, CH_3CN, H_2S, BF_3 and n = 4, 1, 0) with methane.[42]

A similar reaction mechanism describes adequately the first step of the gas-phase hydroxylation of methane catalysed by any of the FeO/EDTA complexes considered here, irrespective of the overall charge of the system. C–H bond breaking was induced by constraining the O(oxo)–H(CH_4) distance to decrease from its value in the optimised encounter complex till the point at which the barrier was overcome (1.1–0.9 Å), and performing a full geometry optimisation for each value of the constrained distance. In general, barriers were found to decrease with increasing protonation number (Table 4), i.e. with increasing positive charge on the encounter complex, varying, at the OPBE (BLYP) level of theory, from 7 (10) kJ mol^{-1} in $[FeO{\cdot}EDTAH_4]^{2+}$–CH_4 to 93 (124) kJ mol^{-1} in $[FeO{\cdot}EDTA]^{2-}$–CH_4. This trend is not simply a manifestation of the stronger electrostatic attraction by an electron as this is being promoted from the substrate donor to the FeO acceptor orbital, because the C–H dissociation involves the simultaneous transfer of one electron *and* one proton (i.e. *a neutral hydrogen atom* H $\uparrow$), and it does not result in a net accumulation of charge on either the FeO or the CH_4 moieties at any time during the course of the reaction. This observation is consistent with the fact that the electron was found to be equally shared between donor and acceptor at the maximum of the barrier, corresponding to the transition state of the C–H bond dissociation. A similar result was also proved to hold to good accuracy in the hydroxylation of methane catalysed by the complexes studied in ref.[42] and in the reactions of $[FeO(H_2O)_5]^{2+}$ with methane and methanol in the gas phase.[43]

The origin of the smaller barrier for positively charged complexes is rather a consequence of the different response of the donor and acceptor orbital to a change in the overall charge of the complex. The ability of a FeO species in a quintet ground state, like $[FeO(H_2O)_5]^{2+}$, to promote hydrogen atom transfer from a substrate is critically influenced by the relative energies of the donor (in this case CH_4 HOMO) and the acceptor (FeO $3\sigma^*\uparrow$) orbitals.[42,43] In all cases studied so far, the energy of the donor orbital was always estimated to be below the one of the acceptor in the encounter complex. This entails that the relative contribution of the donor orbital to the mixed donor-acceptor hybrid orbital responsible for the electron transfer is high, and the electron remains well localised on the substrate. The energy of this orbital increases as the C–H bond is being stretched, and consequently the acceptor orbital character in the charge-transfer orbital is enhanced until donor and acceptor contribute by the same amount to the mixing.[43] After bond breaking (at the transition state) the acceptor orbital contribution becomes dominant, which brings about a progressive localisation of the electron on the catalyst. A consequence of this model is that lowering the energy of the $3\sigma^*\uparrow$ orbital results in a reduced C–H dissociation barrier, as the mixed donor-acceptor orbital in the encounter complex is more similar to the transition state (i.e. the electron is already partially transferred to the catalyst in the encounter complex). In the hypothetical limiting case in which the energy of the donor and acceptor orbitals are the same (or in which the acceptor is below the donor), the C–H dissociation reaction might be expected to occur without an energy barrier. A theoretical realisation of this situation has been described in ref.[42] where we showed that when there is no axial ligand to push the $3\sigma^*\uparrow$ up, as in a hypothetical $[FeO(H_2O)_4]^{2+}$ complex in a constrained square-planar coordination (i.e. in the absence of an axial ligand), C–H bond dissociation of gas-phase CH_4 occurs with a calculated energetic barrier of the order of 1 kJ mol^{-1}.

The energy of the $3\sigma^*\uparrow$ orbital as part of an encounter complex $[FeO{\cdot}EDTAH_n]^{(n-2)+}$–$CH_4$ but in the absence of (orbital) interactions with the substrate can be estimated from a self consistent eigenvalue calculation on $[FeO{\cdot}EDTAH_n]^{(n-2)+}$ constrained in the geometry that it would assume in the encounter complex [Table 4, $\varepsilon_{complex}(3\sigma^*\uparrow)$]. The energy of the donor orbital of CH_4 in

Table 4. Second column: OPBE (BLYP in parenthesis) C–H dissociation barriers (in kJ mol^{-1}) for gas-phase reactions with methane. $\varepsilon_{HOMO,free}(CH_4)$: OPBE energy of the HOMO of an isolated CH_4 molecule constrained to the geometry computed for the optimised encounter complex $[FeO{\cdot}EDTAH_n]^{(n-2)+}$–$CH_4$. $\varepsilon_{HOMO,complex}(CH_4)$: *estimated* OPBE energy of the CH_4 HOMO as part of the encounter complex (see text for details). $\varepsilon_{complex}(3\sigma^*\uparrow)$: energy of the $3\sigma^*\uparrow$ orbital for a $[FeO{\cdot}EDTAH_n]^{(n-2)+}$ complex in the geometry computed for the corresponding $[FeO{\cdot}EDTAH_n]^{(n-2)+}$–$CH_4$ encounter complex. Δ: estimated OPBE energy difference between donor and acceptor (FeO $3\sigma^*\uparrow$) in the encounter complex.

	Reaction barrier	$\varepsilon_{HOMO,free}(CH_4)$	$\varepsilon_{HOMO,complex}(CH_4)$	$\varepsilon_{complex}(3\sigma^*\uparrow)$	Δ
$[FeO{\cdot}EDTA]^{2-}$	93 (124)	–9.328	–4.025	2.301	6.326
$[FeO{\cdot}EDTAH]^{-}$	89 (123)	–9.328	–6.158	–0.414	5.744
$[FeO{\cdot}EDTAH_2]$	90 (106)	–9.347	–8.424	–3.895	4.529
$[FeO{\cdot}EDTAH_3]^{+}$	84 (99)	–9.356	–10.786	–7.513	3.273
$[FeO{\cdot}EDTAH_4]^{2+}$	7 (10)	–9.289	–13.155	–11.598	1.557

the complex, $\varepsilon_{HOMO,complex}(CH_4)$, may be estimated from the corresponding energy in a free CH_4 molecule in the same slightly distorted geometry adopted in the complex $\varepsilon_{HOMO,free}(CH_4)$ and the shift in energy brought about by the presence of the (charged) FeO/EDTA complex. The latter quantity can be calculated from the energy shift of the lowest valence orbital of methane ($2a_1$ in the undistorted tetrahedral symmetry) when the molecule is brought from the gas phase to the encounter complex environment. We verified that in all cases this orbital shows negligible mixing with any other orbital in the complex. Under the assumption that all molecular orbitals are shifted by roughly the same amount when the substrate is included in the encounter complex, this orbital can thus provide an appropriate energy reference. The energy shift varies from ca. +5 eV to about –4 eV as the charge of the complex changes from –2 to +2, and it is nonzero and positive (ca. 1 eV) even in the neutral $[FeO{\cdot}EDTAH_2]$–CH_4 system.

The dependence of the $3\sigma^*\uparrow$ and estimated CH_4 HOMO energies in each encounter complex is shown in Figure 6 as a function of the complex charge. The energy of the CH_4 HOMO shows a linear dependence on the complex charge, decreasing as the charge becomes more positive. This behaviour resembles the response of an orbital energy to a constant shift in the (electrostatic) potential, and appears to be independent of the actual charge distribution within the $[FeO{\cdot}EDTAH_n]^{(n-2)+}$–$CH_4$ complex. Effectively, the latter is seen by the substrate as a spherically symmetric (or point like) charge distribution. Notice that in all complexes the distance between the H atom of methane and the O(oxido) atom does not deviate from an average value of 2.493 Å by more than ca. 0.26 Å (Table 5), and it is therefore almost exclusively the change in the FeO/EDTA complex charge that determines the Coulombic field experienced by the substrate states. The response of the $3\sigma^*\uparrow$ orbital to increasing protonation is by contrast non trivial, and can best be approximated by a parabolic curve with a negative quadratic coefficient. A consequence of this differing dependencies is that the difference between the $3\sigma^*\uparrow$ and the CH_4 HOMO energies (Table 4, Δ), and therefore the C–H dissociation barrier, decreases as the complex charge becomes more positive. It might be estimated by extrapolation that the zero-barrier limit would be reachable for a charge of about +3.

It is interesting to observe that $[FeO{\cdot}EDTAH_4]^{2+}$–CH_4 is the only system among those studied here for which a C–H dissociation barrier lower than for gas-phase $[FeO(H_2O)_5]^{2+}$–CH_4 has been computed, 10 vs. 23 kJ mol^{-1} [23] at the BLYP level of theory (notice the slight difference in the basis set used in the calculations of ref.[43]). As remarked, the electronic structure of $[FeO{\cdot}EDTAH_4]^{2+}$ bears clear analogies with $[FeO(H_2O)_5]^{2+}$. One first important difference is that the gap between the $3\sigma^*\uparrow$ and the $2\pi_x\downarrow$ orbitals is noticeably smaller in $[FeO(H_2O)_5]^{2+}$, where it is 0.334 (BLYP, TZ2P) and 0.725 (OPBE), to be compared to 0.621 (BLYP) and 0.933 eV (OPBE) in $[FeO{\cdot}EDTAH_4]^{2+}$. To the best of our knowledge, all theoretical investigations performed to date on isolate or solvated $[FeO(H_2O)_5]^{2+}$ point to the essentially exclusive involvement of the $3\sigma^*\uparrow$ orbital as an electron acceptor. Based on these observations, we believe that a similar conclusion can be carried over to $[FeO{\cdot}EDTAH_4]^{2+}$, and possibly to FeO/EDTA complexes in different protonation states. The larger $2\pi_x\downarrow - 3\sigma^*\uparrow$ energy difference in $[FeO{\cdot}EDTAH_4]^{2+}$ (the relatively lower energy of the $3\sigma^*\uparrow$) is a manifestation of the much weaker "push" exerted on the $3\sigma^*\uparrow$ by the two nitrogen atoms in the axial region of the ferryl group, compared to the oxygen of the proper axial water ligand in $[FeO(H_2O)_5]^{2+}$. Although a nitrogen lone pair in axial position tends to destabilise the $3\sigma^*\uparrow$ orbital more than an oxygen ligand,[42] the EDTA coordination to FeO^{2+} introduces only two relatively

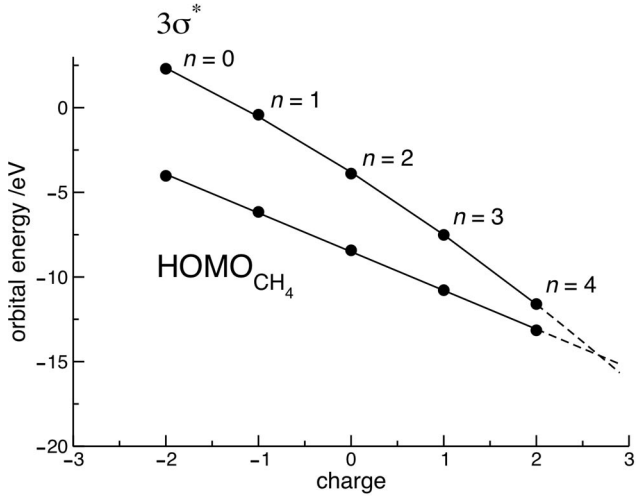

Figure 6. Estimated energies (dots) of the $3\sigma^*\uparrow$ (acceptor) $\varepsilon_{complex}(3\sigma^*\uparrow)$ and CH_4 HOMO (donor) $\varepsilon_{HOMO,complex}(CH_4)$ in $[FeO{\cdot}EDTAH_n]^{(n-2)+}$–$CH_4$ as a function of the complex charge. Protonation numbers (n) are indicated. Continuous lines correspond to quadratic $y = a_0 + a_1x + a_2x^2$ ($3\sigma^*\uparrow$) and linear $y = a_0 + a_1x$ (HOMO CH_4) regression obtained from the calculated points, with coefficients (in appropriate units) $a_0 = -3.81$, $a_1 = -3.49$, $a_2 = -0.20$ and $a_0 = -8.51$, $a_1 = -2.29$, respectively. The dashed lines are extrapolations of the calculated regression curves. Their crossing corresponds to a hypothetical barrierless reaction ($\Delta \approx 0$), and it occurs at charge = +2.7.

Table 5. Selected OPBE-optimised distances (Å) and Fe–O(oxo)–H(CH_4) angle (degrees) for $[FeO{\cdot}EDTAH_n]^{(n-2)+}$–$CH_4$ complexes.

	$[FeO{\cdot}EDTA]^{2-}$–CH_4	$[FeO{\cdot}EDTAH]^{-}$–CH_4	$[FeO{\cdot}EDTAH_2]$–CH_4	$[FeO{\cdot}EDTAH_3]^{+}$–CH_4	$[FeO{\cdot}EDTAH_4]^{2+}$–CH_4
FeO(oxido)	1.620	1.625	1.620	1.617	1.600
O(oxido)–H(CH_4)	2.657	2.235	2.494	2.484	2.589
C–H	1.093	1.093	1.092	1.091	1.095
Fe–O(oxido)–H(CH_4)	173.16	158.46	143.16	146.75	150.43

remote off-axis N ligands. The larger Fe^{IV}–N distances in $[FeO{\cdot}EDTAH_4]^{2+}$ (2.671 Å) compared to the Fe^{IV}–O distance in $[FeO(H_2O)_5]^{2+}$ (2.157 Å) result in an overall reduced destabilisation of the $3\sigma^* \uparrow$ in the first case. The same factor explains the much lower reactivity of the quintet $[FeO(H_2O)_4(NH_3)]^{2+}$ species studied in ref.[42] which is characterised by a substantially *shorter* Fe^{IV}–N distance (2.124 Å) compared to $[FeO{\cdot}EDTAH_4]^{2+}$. The effects of varying Fe^{IV}–N distances on the spin state and spectroscopic properties of oxido-Fe^{IV} compounds has recently been analysed in detail by Neese in the case of the hypothetical gas-phase compound $[FeO(NH_3)_5]^{2+}$.[24] As pointed out in ref.[42] the axial ligand destabilisation of the $3\sigma^* \uparrow$ orbital originates from admixture of axial donor orbital character (σ lone pair of O or N), in the form of an antibonding combination with the Fe^{IV} $3d_{z^2}$ orbital, and this is also observed in the FeO/EDTA complexes examined here (see e.g. upper panel of Figure 5). A linear dependence of the C–H abstraction barrier on the percentage of axial ligand orbital admixture was observed in all the compounds examined in ref.[42] with slope ca. 11.5 kJ mol^{-1} and intercept at origin ca. 0.9 at the BLYP level. Using the total percentage admixture of the two N σ lonepairs in $[FeO{\cdot}EDTAH_4]^{2+}$ (1%) we can then estimate a C–H dissociation barrier of ca. 12.4 kJ mol^{-1}, which is again in good agreement with the BLYP value obtained from constrained dissociation (10 kJ mol^{-1}). The small percentage of σ lone pair admixture is evidently a consequence of the large Fe^{IV}–N distances and possibly of the orientation of the N lonepairs, which deviates noticeably from linearity along the *z* (FeO) axis.

For completeness we briefly discuss the fact, seemingly in contradiction with the previous discussion, that the $3\sigma^* \uparrow$ orbital is at substantially lower energy in $[FeO(NH_3)_5]^{2+}$ (–13.781 eV, BLYP (TZ2P); –14.138 eV, OPBE) than in $[FeO{\cdot}EDTAH_4]^{2+}$ (–11.361 eV, BLYP; –11.598 eV, OPBE), while the C–H dissociation in $[FeO{\cdot}EDTAH_4]^{2+}$–CH_4 proceeds with a noticeably lower barrier. One would rather expect the barrier to decrease with the lower $3\sigma^* \uparrow$ energy, since the lower the energy of the latter, the higher is its affinity for the electron from the substrate HOMO. However, as was hinted at in ref.[43] and as we have confirmed here, the dissociation barrier should rather be related to the $3\sigma^* \uparrow$ energy relative to the energy of the donor orbital *in the encounter complex*. Although $[FeO{\cdot}EDTAH_4]^{2+}$–CH_4 and $[FeO(H_2O)_5]^{2+}$–CH_4 carry the same positive charge, and therefore both stabilise the substrate orbital energies relative to the free reactant, the equilibrium geometries of the two complexes differ. In particular, the O(oxo)–H(CH_4) distances are 2.589 and 1.606 Å, respectively, and CH_4 therefore experiences a much stronger electrostatic field when in $[FeO(H_2O)_5]^{2+}$–CH_4. A reliable estimate of the parameter Δ could not be obtained for this system, but it is reasonable to expect that the donor orbital of CH_4 would be stabilised to a value of Δ larger than in $[FeO{\cdot}EDTAH_4]^{2+}$–CH_4, thus resulting in a larger barrier. Our conclusion is that, although the absolute energy of the $3\sigma^* \uparrow$ can be used as a rough index of FeO reactivity, caution should be taken when comparing different reactant complex geometries, or when different substrates are considered.

Conclusions

We have described an analysis of the geometry and electronic structure of a series of ferryl compounds of composition $[FeO{\cdot}EDTAH_n]^{(n-2)+}$ (n = 0, 1, 2, 3, 4), and of their ability to promote C–H activation in methane in the gas phase. All compounds were found to possess a quintet ground state, only slightly more stable than the triplet state, in close analogy with (gas phase) $[FeO(H_2O)_5]^{2+}$. Intermediate protonation numbers (n = 1–3) were found to give rise to more stable complexes, likely as a balance of ligand distortion, electrostatic and orbital interaction effects. Similar to $[FeO(H_2O)_5]^{2+}$, the C–H activation properties of all complexes were found to be dominated by a low lying $3\sigma^* \uparrow$ orbital, acting as an acceptor of one electron during a transfer of a hydrogen atom from methane.

In all ligand protonation states, the systems examined showed remarkable C–H activation properties, with abstraction barriers from CH_4 ranging from about 100 (n = 0) to ca. 10 (n = 4) kJ mol^{-1}. According to our results, the fully protonated dipositive $[FeO{\cdot}EDTAH_4]^{2+}$ complex, which may in principle be present in non negligible concentrations in aqueous solution at very low *p*H,[76] could act as a hydroxylation catalyst with an efficiency comparable if not superior to $[FeO(H_2O)_5]^{2+}$. In fact, the $EDTAH_4$ ligand realizes the requirements for an effective ligand for hydroxylation activity of FeO^{2+}, namely weak equatorial ligand field (to yield a quintet spin state with ensuing low energy of the $3\sigma^* \uparrow$), high positive charge, and weak axial ligand field. The present findings for the axial ligation by EDTA agree *at a quantitative level* with the results of ref.[42] in which a correlation was established between the donor properties of the axial (i.e. *trans* to the oxo ion relative to the Fe^{IV}) ligand and the C–H activation properties of a oxido-Fe^{IV} system. In particular, we prove here that remote N ligands in axial position exert only a negligible "push" on the $3\sigma^* \uparrow$ orbital, effectively leaving the axial region of the oxido-Fe^{IV} moiety essentially non coordinated. Work is in progress to establish whether a similar situation may occur at ambient conditions in aqueous solution.

Although no conclusive evidence has been put forward to date as to the involvement of ferryl species in oxygenated Fe^{II}/EDTA chemistry, our results suggest that chelated FeO^{2+} systems with a *quintet* ground state and reactivity analogous to the alleged "Fenton catalyst" $[FeO(H_2O)_5]^{2+}$ may be generated in conditions easily accessible experimentally. As such, they may provide access to new classes of highly efficient and comparatively inexpensive catalysts for alkane hydroxylations at room temperature and pressure conditions.

Supporting Information (see also the footnote on the first page of this article): Optimised geometrical coordinates, spin densities and

atomic charges of all the reaction species and transition states; energies along reaction pathways for all reactions considered; transition vectors and frequency analysis for the transition state of the reaction of $[FeO{\cdot}EDTAH_4]^{2+}$ with CH_4.

Acknowledgments

This work was supported by the Dutch National Research School Combination "Catalysis by Design" (NRSC-C). Computer resources were provided by the Netherlands' Scientific Research Council (NOW) through a grant from the Stichting Nationale Computerfaciliteiten (NCF).

[1] A. Ghosh, *J. Inorg. Biochem.* **2006**, *100*, 419–420.
[2] G. T. Babcock, *Proc. Natl. Acad. Sci. USA* **1999**, *96*, 12971–12973.
[3] T. Omura, *Biochem. Biophys. Res. Commun.* **1999**, *266*, 690–698.
[4] W. L. Smith, D. L. DeWitt, R. M. Garavito, *Annu. Rev. Biochem.* **2000**, *69*, 145–182.
[5] F. D'Agnillo, A. I. Alayash, *Free Radiat. Biol. Med.* **2002**, *33*, 1153–1164.
[6] R. K. Behan, M. T. Green, *J. Inorg. Biochem.* **2006**, *100*, 448–459.
[7] A. V. Nemukhin, I. A. Topol, R. E. Cachau, S. K. Burt, *Theor. Chem. Acc.* **2006**, *115*, 348–353.
[8] J. T. Groves, *J. Inorg. Biochem.* **2006**, *100*, 434–447.
[9] A. Bassan, M. R. A. Blomberg, T. Borowski, P. E. M. Siegbahn, *J. Inorg. Biochem.* **2006**, *100*, 727–743.
[10] P. G. Debrunner, *Hyperfine Interact.* **1990**, *53*, 21–36.
[11] R. Rutter, M. Valentine, M. P. Hendrich, L. P. Hager, P. G. Debrunner, *Biochemistry* **1983**, *22*, 4769–4774.
[12] R. Rutter, L. P. Hager, H. Dhonau, M. Hendrich, M. Valentine, P. Debrunner, *Biochemistry* **1984**, *23*, 6809–6816.
[13] C. E. Schulz, P. W. Devaney, H. Winkler, P. G. Debrunner, N. Doan, R. Chiang, R. Rutter, L. P. Hager, *FEBS Lett.* **1979**, *103*, 102–105.
[14] C. E. Schulz, R. Rutter, J. T. Sage, P. G. Debrunner, L. P. Hager, *Biochemistry* **1984**, *23*, 4743–4754.
[15] H.-P. Hersleth, U. Ryde, P. Rydberg, C. H. Görbitz, K. K. Andersson, *J. Inorg. Biochem.* **2006**, *100*, 460–476.
[16] J.-U. Rohde, L. Que Jr, *Angew. Chem. Int. Ed.* **2005**, *44*, 2255–2258.
[17] J.-U. Rohde, J.-H. In, M. H. Lim, W. W. Brennessel, M. R. Bukowski, A. Stubna, E. Münck, W. Nam, L. Que Jr, *Science* **2003**, *299*, 1037–1039.
[18] J. Kaizer, E. J. Klinker, N. Y. Oh, J.-U. Rohde, W. J. Song, A. Stubna, J. Kim, E. Münck, W. Nam, L. Que Jr, *J. Am. Chem. Soc.* **2003**, *126*, 472–473.
[19] X. Shan, L. Que Jr, *J. Inorg. Biochem.* **2006**, *100*, 421–433.
[20] M. M. Conradie, J. Conradie, A. Ghosh, *J. Inorg. Biochem.* **2006**, *100*, 620–626.
[21] E. J. Klinker, J. Kaizer, W. W. Brennessel, N. L. Woodrum, C. J. Cramer, L. Que Jr, *Angew. Chem. Int. Ed.* **2005**, *44*, 3690–3694.
[22] M. R. Bukowski, K. D. Koehntop, A. Stubna, E. L. Bominaar, J. A. Halfen, E. Münck, W. Nam, L. Que Jr, *Science* **2005**, *310*, 1000–1002.
[23] J. C. Schöneboom, F. Neese, W. Thiel, *J. Am. Chem. Soc.* **2005**, *127*, 5840–5853.
[24] F. Neese, *J. Inorg. Biochem.* **2006**, *100*, 716–726.
[25] F. Buda, B. Ensing, M. C. M. Gribnau, E. J. Baerends, *Chem. Eur. J.* **2001**, *7*, 2775–2783.
[26] A. Ghosh, E. Tangen, H. Ryeng, P. R. Taylor, *Eur. J. Inorg. Chem.* **2004**, *23*, 4555–4560.
[27] A. Bassan, M. R. A. Blomberg, P. E. M. Siegbahn, *Chem. Eur. J.* **2003**, *9*, 106–115.
[28] F. Buda, B. Ensing, M. C. M. Gribnau, E. J. Baerends, *Chem. Eur. J.* **2003**, *9*, 3436–3444.
[29] A. Decker, J.-U. Rohde, L. Que Jr, E. I. Solomon, *J. Am. Chem. Soc.* **2004**, *126*, 5378–5379.
[30] S. Shaik, M. Filatov, D. Schröder, H. Schwarz, *Chem. Eur. J.* **1998**, *4*, 193–199.
[31] N. Harris, S. Shaik, D. Schröder, H. Schwarz, *Helv. Chim. Acta* **1999**, *82*, 1784–1797.
[32] D. Schröder, S. Shaik, H. Schwarz, *Acc. Chem. Res.* **2000**, *33*, 139–145.
[33] H. Hirao, D. Kumar, L. Que Jr, S. Shaik, *J. Am. Chem. Soc.* **2006**, *128*, 8590–8606.
[34] T. Løgager, J. Holcman, K. Sehested, T. Pedersen, *Inorg. Chem.* **1992**, *31*, 3523–3529.
[35] O. Pestovsky, A. Bakac, *J. Am. Chem. Soc.* **2004**, *126*, 13757–13764.
[36] O. Pestovsky, S. Stoian, E. L. Bominaar, X. Shan, E. Münck, L. Que Jr, A. Bakac, *Angew. Chem. Int. Ed.* **2005**, *44*, 6871–6874.
[37] P. Wardman, L. P. Candeias, *Radiat. Res.* **1996**, *145*, 523–531.
[38] H. B. Dunford, *Coord. Chem. Rev.* **2002**, *233*, 311–318.
[39] F. Gozzo, *J. Mol. Catal. A Chem.* **2001**, *171*, 1–22.
[40] M. L. Kremer, *Phys. Chem. Chem. Phys.* **1999**, *15*, 3595–3605.
[41] B. Ensing, F. Buda, P. Blöchl, E. J. Baerends, *Phys. Chem. Chem. Phys.* **2002**, *4*, 3619–3627.
[42] L. Bernasconi, M. J. Louwerse, E. J. Baerends, *Eur. J. Inorg. Chem.* **2007**, 3023–3033.
[43] M. J. Louwerse, E. J. Baerends, *Phys. Chem. Chem. Phys.* **2007**, *9*, 156–166.
[44] A. Decker, M. D. Clay, I. Solomon, *J. Inorg. Biochem.* **2006**, *100*, 697–706.
[45] J. T. Groves, M. Van Der Puy, *J. Am. Chem. Soc.* **1974**, *96*, 5274–5275.
[46] J. T. Groves, G. A. McClusky, *J. Am. Chem. Soc.* **1976**, *98*, 859–861.
[47] K. Yoshizawa, *Acc. Chem. Res.* **2006**, *39*, 375–382.
[48] J. D. Englehardt, D. E. Meeroff, L. Eschegoyen, F. M. Raymo, T. Shibata, *Environ. Sci. Technol.* **2007**, *41*, 270–276.
[49] K. D. Welch, T. Z. Davis, S. D. Aust, *Arch. Biochem. Biophys.* **2002**, *397*, 360–369.
[50] C. E. Noradoun, I. F. Cheng, *Environ. Sci. Technol.* **2005**, *39*, 7158–7163.
[51] V. Zang, R. van Eldik, *Inorg. Chem.* **1990**, *29*, 1705–1711.
[52] S. Seibig, R. van Eldik, *Inorg. Chem.* **1997**, *36*, 4115–4120.
[53] B. Ensing, F. Buda, P. Blöchl, E. J. Baerends, *Angew. Chem. Int. Ed.* **2001**, *40*, 2893–2895.
[54] L. Bernasconi, E. J. Baerends, manuscript in preparation.
[55] S. V. Kryatov, E. V. Rybak-Akimova, S. Schindler, *Chem. Rev.* **2005**, *105*, 2175–2226.
[56] E. I. Solomon, T. C. Brunold, M. I. Davis, J. N. Kemsley, S.-K. Lee, N. Lehnert, F. Neese, A. J. Skulan, Y.-S. Yang, J. Zhou, *Chem. Rev.* **2000**, *100*, 235–349.
[57] R. L. Lieberman, A. C. Rosenzweig, *Nature* **2005**, *34*, 177–182.
[58] P. E. M. Siegbahn, R. H. Crabtree, P. Nordlund, *J. Biol. Inorg. Chem.* **1998**, *3*, 314–317.
[59] P. E. M. Siegbahn, *Inorg. Chem.* **1999**, *38*, 2880–2889.
[60] P. E. M. Siegbahn, *J. Biol. Inorg. Chem.* **2001**, *6*, 27–45.
[61] T. Lind, P. E. M. Siegbahn, R. H. Crabtree, *J. Phys. Chem. B* **1999**, *103*, 1193–1202.
[62] ADF2005.01, SCM, Theoretical Chemistry, Vrije Universiteit Amsterdam, The Netherlands; http://www.scm.com.
[63] E. J. Baerends, D. E. Ellis, P. Ros, *Chem. Phys.* **1973**, *2*, 41–51.
[64] C. Fonseca Guerra, J. G. Snijders, G. te Velde, E. J. Baerends, *Theor. Chem. Acc.* **1998**, *99*, 391–403.
[65] E. van Lenthe, E. J. Baerends, J. G. Snijders, *J. Chem. Phys.* **1994**, *101*, 9783–9792.
[66] A. Becke, *Phys. Rev. A* **1988**, *38*, 3098–3100.
[67] C. Lee, W. Yang, R. G. Parr, *Phys. Rev. B* **1988**, *37*, 785–789.
[68] N. C. Handy, A. J. Cohen, *Mol. Phys.* **2001**, *99*, 403–412.
[69] J. P. Perdew, K. Burke, M. Ernzerhof, *Phys. Rev. Lett.* **1996**, *77*, 3865–3868.

[70] A. Fouqueau, S. Mer, M. E. Casida, L. M. L. Daku, A. Hauser, T. Mineva, F. Neese, *J. Chem. Phys.* **2004**, *120*, 9473–9486.
[71] A. Fouqueau, M. E. Casida, L. M. L. Daku, A. Hauser, F. Neese, *J. Chem. Phys.* **2005**, *122*, 044110.
[72] M. Swart, A. R. Groenhof, A. W. Ehlers, K. Lammertsma, *J. Phys. Chem. A* **2004**, *108*, 5479–5483.
[73] A. R. Groenhof, M. Swart, A. W. Ehlers, K. Lammertsma, *J. Phys. Chem. A* **2005**, *109*, 3411–3417.
[74] N. Lehnert, R. Y. N. Ho, L. Que Jr, E. I. Solomon, *J. Am. Chem. Soc.* **2001**, *123*, 8271–8290.
[75] B. Ensing, F. Buda, M. C. M. Gribnau, E. J. Baerends, *J. Am. Chem. Soc.* **2004**, *126*, 4355–4365.
[76] pK_a values for the uncoordinated EDTA ligand have been reported[51] of 1.99, 2.67, 6.16, 10.26.

Received: October 18, 2007
Published Online: February 11, 2008

